HHS Public Access

Author manuscript

Mol Cancer Ther. Author manuscript; available in PMC 2018 September 01.

Published in final edited form as:

Mol Cancer Ther. 2017 September ; 16(9): 1779–1790. doi:10.1158/1535-7163.MCT-16-0848.

Inhibition of Hsp90 suppresses PI3K/AKT/mTOR signaling and has antitumor activity in Burkitt lymphoma

Lisa Giulino-Roth[1,2], **Herman J. van Besien**[2], **Tanner Dalton**[2], **Jennifer E. Totonchy**[2], **Anna Rodina**[3], **Tony Taldone**[3], **Alexander Bolaender**[3], **Hediye Erdjument-Bromage**[6,*], **Jouliana Sadek**[2], **Amy Chadburn**[2], **Matthew J. Barth**[4], **Filemon S. Dela Cruz**[5], **Allison Rainey**[5], **Andrew L. Kung**[5], **Gabriela Chiosis**[3], and **Ethel Cesarman**[2]

[1]Department of Pediatrics, Weill Cornell Medical College, New York, NY

[2]Department of Pathology and Laboratory Medicine, Weill Cornell Medical College, New York, NY

[3]Program in Chemical Biology, Memorial Sloan Kettering Cancer Center, New York, NY

[4]Department of Pediatrics, Roswell Park Cancer Institute, Buffalo, NY

[5]Department of Pediatrics, Memorial Sloan Kettering Cancer Center, New York, NY

[6]Molecular Biology Program, Memorial Sloan Kettering Cancer Center, New York, NY

Abstract

Heat shock protein 90 (Hsp90) is a molecular chaperone that protects proteins, including oncogenic signaling complexes, from proteolytic degradation. PU-H71 is a next-generation Hsp90 inhibitor that preferentially targets the functionally distinct pool of Hsp90 present in tumor cells. Tumors that are driven by the MYC oncoprotein may be particularly sensitive to PU-H71 due to the essential role of Hsp90 in the epichaperome which maintains the malignant phenotype in the setting of MYC. Burkitt lymphoma (BL) is an aggressive B-cell lymphoma characterized by MYC dysregulation. In the current study we evaluated Hsp90 as a potential therapeutic target in Burkitt lymphoma. We found that primary BL tumors overexpress Hsp90 and that Hsp90 inhibition has anti-tumor activity *in-vitro* and *in-vivo*, including potent activity in a patient derived xenograft model of BL. To evaluate the targets of PU-H71 in BL we performed high affinity capture followed by proteomic analysis using mass spectrometry. We found that Hsp90 inhibition targets multiple components of PI3K/AKT/mTOR signaling, highlighting the importance of this pathway in BL. Lastly, we found that the anti-lymphoma activity of PU-H71 is synergistic with dual PI3K/mTOR inhibition *in-vitro* and *in-vivo*. Overall this work provides support for Hsp90 as a therapeutic target in BL and suggests the potential for combination therapy with PU-H71 and inhibitors of PI3K/mTOR.

Corresponding Author: Lisa Giulino Roth, 525 East 68th Street, Payson 695, New York, NY 10065, lgr2002@med.cornell.edu Phone: (212) 746-3494, Fax: (212) 746-8609.

*Current Affiliation: Department of Biochemistry and Molecular Pharmacology, New York University School of Medicine, Skirball Institute, New York, NY

Introduction

Burkitt lymphoma (BL) is a germinal center B-cell derived malignancy that is molecularly characterized by the translocation of the *MYC* proto-oncogene to either the immunoglobulin heavy or the κ or λ light chains. Beyond the *MYC* translocation, Burkitt lymphoma is heterogeneous from a genomic standpoint. Recurrent somatic alterations have recently been described in *TP53* (approximately 50% of cases); *TCF3* or its negative regular *ID3* (34–70% of cases); *CCND3* (38% of cases); and the SWI/SNF family of chromatin remodeling genes (17–43% of cases)(1–4). Novel therapies are needed in Burkitt lymphoma where the survival for patients with relapsed disease is <20%(5,6). One approach to therapeutic targeting in BL given the molecular heterogeneity is to focus on global mechanisms of lymphomagenesis, which are independent of genetic subtype.

The heat shock protein 90 (Hsp90) has emerged as a desirable target in cancer due to its role in the regulation of pathways required for malignant growth(7). Hsp90 is an ATP-dependent molecular chaperone that protects proteins from proteolytic degradation including oncogenic signaling complexes. Inhibitors that broadly target Hsp90, however, have been limited in their clinical development due to suboptimal target inhibition and off-target toxicities. More recent studies have elucidated a biochemically distinct Hsp90 complex in cancer cells that is unique from the fraction of Hsp90 engaged in housekeeping functions(8). This “tumor-enriched” Hsp90 is amenable to small molecule inhibition. PU-H71 is a purine scaffold Hsp90 inhibitor with preferential uptake in tumor tissue and selective binding to the tumor-enriched fraction of Hsp90(9). PU-H71 specifically targets oncogenic Hsp90 clients, for example: Bcr-Abl but not cellular Abl; mutated, but not WT mB-Raf; and the aberrantly activated signaling complex containing Bcl6(8,10). This agent, as well as other inhibitors of Hsp90, are currently being evaluated in phase I and phase II clinical trials (clinicaltrials.gov ID: NCT01393509, NCT02261805, NCT02474173).

More recently, a chaperome network (coined the epichaperome) was identified in a subset of cancers, and found to be specifically targeted by PU-H71 (11). This epichaperome appears to rely on dysregulated MYC, and is present in tumors that overexpress the MYC oncoprotein. While Burkitt lymphoma is characterized by MYC translocation and deregulation, the Hsp90 chaperome and the effects of PU-H71 have not been studied in Burkitt lymphoma. In the current study we evaluated Hsp90 as a therapeutic target in BL. We hypothesized that Hsp90 inhibition would disrupt oncogenic client proteins required for BL survival. We found that Hsp90 inhibition has anti-lymphoma effects *in-vitro* and *in-vivo*, including activity in a patient derived xenograft model of BL. In order to determine the relevant Hsp90 clients in BL and thereby define the Hsp90 oncoproteome, we used PU-H71 affinity capture and proteomics(8,12). We identified multiple components in the PI3K/AKT/mTOR signaling pathway as Hsp90 clients in BL. In addition we found that Hsp90 inhibition was synergistic with PI3K/mTOR inhibition. Collectively, these results support Hsp90 as a rational therapeutic target in BL and identify a novel strategy for combination therapy.

Materials and Methods

Cell culture, immunoblot, and reagents

Ramos, Raji, Namalwa, Daudi, CA-46, Ly10 and Ly18 cell lines were purchased from American Type Culture Collection (ATCC) in 2013. Jiyoye and DG-75 were purchased from ATCC in 2014. Raji 2R and Raji 4RH were provided by Roswell Park Cancer Institute (M.J.B.). All cells were used for experiments within 2 months of thawing. Cell line characterization was performed by Idex Bioresearch (Westbrook, Maine) using short tandem repeat profiling and multiplex PCR to report cell line characterization and interspecies contamination. Testing was last performed in February 2014. Cells were cultured in RPMI-1640 media (Invitrogen) supplemented with 10% heat inactivated fetal bovine serum and gentamicin 50ug/mL (Sigma-Aldrich). PU-H71, PU-H71-beads, and control beads were synthesized and prepared at Memorial Sloan Kettering Cancer Center as previously reported(13,14). Idelalisib (CAL-101), IPI-145, BKM120 (15), BEZ-235 (16), ganetespib (17), and BIIB-021 (18) were purchased from Selleck Chemicals. MPC-3100 (19) and CUDC-305 (20) were purchased from Santa Cruz and ChemieTek respectively. The chemical structures for PU-H71 and BEZ-235 are presented in Supplemental Figure 1.

Immunoblot, Immunohistochemistry, and tissue microarray (TMA) construction

Cell lysis and immunoblot were performed by standard procedure using the following antibodies: GAPDH (Genetex); p110δ and p110α (Santa Cruz); p110β and p85α (Abcam); PARP (BD Pharmingen); AKT, p110δ, p110β, eIF4E (Cell Signaling Technology), PARP (Santa Cruz), RB and pRB (Cell Signaling Technology). Immunohistochemistry was performed using the following antibodies: Hsp90 (Enzo Life Sciences) p-4EBP1 (BD Pharmingen), BCL2 (Cell Marque), BCL6 (Dako), Ki67 (Dako), TUNEL (prepared as previously described (21)). A TMA was constructed using 0.6mm cores obtained from formalin-fixed paraffin embedded BL tumor samples. Each case was represented on the TMA in duplicate. Quantification of immunohistochemistry was performed using the Halo® image analysis software program (Indica Labs).

Cell viability assays, IC50 calculation and combination studies

Cell viability was determined using trypan blue staining and an ATP based luminescent assay (CellTiter-Glo, Promega). Luminescence was measured using the GloMax® Multi+ Detection System (Promega). IC50 values were calculated using Prism 6 software. For combination treatments, cells were exposed to increasing doses of each drug alone or the combination at a constant ratio in 96-well plates. Cell viability was measured and normalized to vehicle control. Compusyn software (Biosoft) was used to plot dose effect curves and calculate CI value. To evaluate cell viability in GC B-cells, lymphocytes were extracted from de-identified primary human tonsil specimens which were obtained after routine tonsillectomy. Total lymphocytes were treated with PU-H71 in RPMI containing 20% FBS and 100μg/ml Primocin and cultured for 24 hours on gamma-irradiated mouse L CDw32 feeder cells. At indicated times post-treatment lymphocyte cultures were incubated with fixable viability stain (FVS, BD Cat# 564406). Cells were pelleted and resuspended in 100μl cold PBS without calcium and magnesium containing 5% FBS, and 0.1% Sodium Azide (FACS Block) and incubated on ice for 15 minutes after which 100μl cold PBS

containing 0.5% FBS and 0.1% Sodium Azide (FACS Wash) was added. Cells were pelleted and resuspended in FACS Wash containing B cell phenotype panel as follows: Ig Lambda CD19-PE (BD Cat# 240720), CD38-PECy7 (BD Cat# 560667), IgD-PerCP Cy5.5 (BD Cat# 561315), CD27-APC H7 (BD Cat# 560222). Parallel cultures of Ramos treated with PU-H71 and stained only with FVS were included as positive control. Data was acquired on a BD LSR2 Flow Cytometer and analyzed using FlowJo software. Data reported for primary tonsil specimens are the percentage of CD19+ lymphocytes which were both germinal center cells ($CD38^{hi}$, IgD^{low}) and viable (FVS−).

Flow Cytometry for Apoptosis and Cell Cycle Analysis

Cells were treated as indicated and 5×10^5 cells were harvested by centrifugation at indicated timepoints, washed once in PBS and resuspended in 1× AnnexinV staining buffer (BD cat# 556454) containing 3μl/test AnnexinV-AlexaFluor647 (ThermoFisher A23204) and 5μl/test 7-AAD (BD cat# 559925) and incubated at room temperature for 15 minutes. Data was acquired with a BD LSR2 analytical flow cytometer and analyzed using FlowJo software. Necrotic cells were defined as annexin V+/7AAD+ or annexinV−/AAD+ and early apoptotic cells were defined as annexin V+/7AAD−. *Cell Cycle Analysis:* Cells were treated as indicated and 5×10^5 cells were harvested by centrifugation, washed once in PBS and resuspended in 1× Transcription Factor Fix/Perm buffer and incubated for 50 minutes on ice. An equal volume of 1× Perm/Wash buffer was added and cells were pelleted and washed once more in 1× Perm/Wash. Buffers for this procedure were purchased from BD (Cat #562725). Ki67 staining was performed overnight at 4°C in 1× Perm/Wash using 0.5μl Ki67-BV510/test (BD cat# 563462). After staining cells were washed twice with 1× Perm/Wash and resuspended in PBS containing 5μl/test Propidium Iodide (BD Cat#556463). Data was acquired with a BD LSR2 analytical flow cytometer, analyzed using FlowJo software and plotted using the ggplot2 package in R.

PU-H71 affinity capture

Affinity capture and proteomics analysis were performed as previously described(8). Briefly, cells were lysed by collecting them in Felts buffer (20 mM HEPES, 50 mM KCl, 5 mM MgCl2, 0.01% (w/v) NP-40, freshly prepared 20 mM Na2MoO4 (pH 7.2–7.3)) with added 1μg/μl protease inhibitors (leupeptin and aprotinin), followed by three successive freeze (in dry ice) and thaw steps. Total protein concentration was determined using the BCA kit (Pierce) according to the manufacturer's instructions. The PU-H71 conjugated beads were added at a volume of 80μl to the cell lysate (1mg), and the mixture incubated at 4 °C for 4h. The beads were washed five times with Felts lysis buffer and separated by SDS-PAGE, followed by a standard western blotting procedure. Proteins identification was then performed by liquid chromatography coupled to tandem mass spectrometry (LC-MS/MS) as follows: Purified PU-H71 interacting protein complexes were resolved using SDS-polyacrylamide gel electrophoresis, followed by brief staining with Simply Blue (Life Technologies, CA) and excision of the separated protein bands. In situ trypsin digestion of polypeptides in each gel slice was performed and the tryptic peptides were resolved on a nano-capillary reverse phase column. Peptides were directly infused into a linear ion-trap mass spectrometer (LTQ Orbitrap XL, Thermo Electron Corp.). The mass spectrometer was set to collect one survey scan (MS1), followed by MS/MS spectra on the 9 most intense ions

observed in the MS1 scan. Proteins were identified by searching the tandem mass spectra against a human segment of Uniprot protein database (20,273 sequences; European Bioinformatics Institute, Swiss Institute of Bioinformatics and Protein Information Resource) using Mascot search engine (Matrix Science, London, UK; version 2.5.0; www.matrixscinece.com) Decoy database search was always activated and, in general, for merged LC-MS/MS analysis of a gel lane with $p<0.01$, false discovery rate averaged around less than 1%. Scaffold (Proteome Software, Inc., Portland, OR), version 4_4_1 was used to further validate and cross-tabulate tandem mass spectrometry (MS/MS) based protein and peptide identifications.

Cell line xenografts

Six to eight week old male non-obese diabetic/severe combined immunodeficiency (NOD-SCID) mice obtained from Jackson Laboratory were injected in the subcutaneous flank with 1×10^7 Namalwa or Ramos cells in PBS. Mice were evaluated daily for weight and tumor measurement. A 7.5 mg/mL PU-H71 solution was prepared in a 10 mM phosphate buffered solution and delivered via intraperitoneal injection. A 5 mg/mL BEZ-235 solution was prepared in 1:9 N-methylpyrrolidone:polyethylene glycol and delivered via oral gavage. Tumor volumes were measured daily with calipers and tumor volume was calculated as ½ length × width^2. Area under the curve (22) was used to measure tumor volume over time (GraphPad Prism software). Mice were sacrificed when tumors reached a volume of 3000mm^3 or at the completion of the observation period (15 days). Tumors were harvested after animals were sacrificed and sectioned for IHC staining.

Patient derived xenograft

Patient derived xenografts (PDXs) were established by implanting fresh tumor fragments in the subcutaneous flanks of NOD-SCID interleukin-2R gamma null (NSG) mice (n=3). Tumor formation was monitored weekly by inspection and measurement using calipers. When the tumors reached a volume of 1000–1500 mm^3, the PDX tumors were collected after humane euthanasia. The tumors were sectioned into 2mm fragments and implanted into additional animals for subsequent drug testing.

Statistics—Two-tailed unpaired *t* test was used unless otherwise specified. Survival estimates were calculated using Kaplan-Meier analysis. All statistical analyses were carried out using Prism software (GraphPad).

Study Approval—De-identified patient samples were obtained under approval from the Institutional Review Board (23) of Weill Cornell Medical College. The Research Animal Resource Center of Weill Cornell Medical College approved cell line xenograft studies. Patient derived xenograft studies were conducted at Columbia University under the approval of the Columbia University Institutional Animal Care and Use Committee.

Results

Hsp90 is overexpressed in primary Burkitt lymphoma tumors

Hsp90 is ubiquitously expressed in human cells and is upregulated in conditions of chronic cellular stress including disease states and cancer (24). Hsp90 is overexpressed in a variety of cancer subtypes and overexpression has been linked to more aggressive disease and resistance to chemotherapy (25,26). To assess the potential for Hsp90 as a therapeutic target in Burkitt lymphoma, we first evaluated Hsp90 expression in primary human BL tumors. Immunohistochemistry for Hsp90 was performed on a Burkitt lymphoma tissue microarray containing 59 primary tumors and tonsil tissue for control. Fifty-three of 59 cases (90%) demonstrated high levels of Hsp90 expression defined as >90% tumor cell positivity. Quantification of Hsp90 by mean optical density demonstrated a significant increase in expression over normal tonsil (0.673 vs. 0.275, p=0.001) (Figure 1A–B). In Hsp90 + tumors, non-malignant infiltrating cells were negative for Hsp90 (representative images shown in Fig 1B). Since the cell of origin for BL is the germinal center B-cell (27), we also examined Hsp90 expression in normal GC cells in tonsil and lymph node specimens where GCs could be visualized and staining of both tumor and GC cells was performed on the same slide. GC B-cells demonstrated moderate Hsp90 expression relative to high expression seen in BL tumors (Supplemental Fig. 2).

Hsp90 inhibition induces growth arrest in human Burkitt lymphoma cell lines

Although BL tumors were found to express high levels of Hsp90, total amount of this chaperone protein does not necessarily reflect cellular dependency on this protein or sensitivity to Hsp90 inhibitors (11). To determine the sensitivity of BL to Hsp90 inhibition we performed *in-vitro* viability assays with the ATP-based CellTiter-Glo® assay in 9 human BL cell lines (Ramos, DG-75, Raji, Namalwa, Daudi, Jiyoye, CA-46, Raji 2R, and Raji 4RH) and two DLBCL cell lines known to be sensitive to PU-H71 (Ly10, Ly18) (Figure 1C, Supplemental Figure 3A). Cells were exposed to increasing concentrations of PU-H71 and viability was assessed at 24, 48, and 72 hours. All cell lines demonstrated time and dose dependent growth inhibition. Results were confirmed by evaluating cell viability with trypan blue (Supplemental Figure 3B). The concentration of PU-H71 that inhibited viability by 50% (IC50) was in the nanomolar range (171–337nM) and was consistent across cell lines. The Raji 2R and Raji 4RH cell lines which have acquired resistance to rituximab and multiple chemotherapeutic agents (28) were equally sensitive to PU-H71 (IC50 175–181nM). To determine if PU-H71 was broadly toxic to GC B-cells we exposed primary human tonsil tissue to PU-H71 and evaluated viability in GC B-cells using flow cytometry. Ramos cells but not GC B-cells demonstrated substantial reduction in viability upon exposure to PU-H71 (Supplemental Figure 3C). To determine if the effect on BL growth was unique to PU-H71, we tested four additional small molecule Hsp90 inhibitors in BL cells: BIIB-021, CUDC-305, ganetespib, and MPC-3100 (17–20) (Figure 1D). Cells were sensitive to all four Hsp90 inhibitors with IC50 ranging from 3.8–149.5 nM. This work demonstrates that BL is broadly sensitive to Hsp90 inhibition.

Given data from our group that Hsp90 inhibition may preferentially target gamma herpesvirus-associated malignancies (29), we included both EBV-positive (n=4) and EBV-

negative (n=3) subtypes of BL in our PU-H71 screen including both the sporadic and endemic forms of BL (Figure 1C). There was no difference in sensitivity in EBV-positive and EBV-negative cells (IC50 290 and 217 nM respectively, p=0.239). This suggests that the mechanism of action of PU-H71 is independent of EBV-mediated oncogenesis in BL. This may be explained by the restricted EBV latency observed in BL where few viral proteins are expressed and are not major oncogenic drivers (30).

To determine the mechanism of growth inhibition, we evaluated the effect of treatment on cell cycle using flow cytometry and PI/Ki67 staining (Figure 2A). Cell cycle analysis revealed an accumulation of cells in G0 upon treatment with PU-H71, suggesting that PU-H71 inhibits the growth of BL primarily through cell cycle arrest. An evaluation of apoptosis using flow cytometry and Annexin V/7AAD staining revealed an increase in necrotic cells (annexin V+/7AAD+ or annexinV−/7AAD+) by 72 hours of treatment, but no corresponding increase in early apoptotic cells (annexinV+/7AAD−) at any timepoint (Figure 2B). Moreover, we did not observe PARP cleavage as measured by western blot (Figure 2C) or increases in caspase 3 or 7 activity as measured by the fluorescent assay Caspase-Glo® (Figure 2D) consistent with a non-apoptotic mechanism of cell death. This is also supported by a lack of increase in the sub-G0 population in the cell cycle analysis, which reflects DNA fragmentation and is characteristic of apoptotic cell death. Based on this we conclude that PU-H71 induces cell cycle arrest in BL followed by non-apoptotic cell death.

Hsp90 inhibition delays tumor growth and prolongs survival *in-vivo*

To determine the anti-lymphoma effect of Hsp90 inhibition *in vivo* we established Namalwa xenografts in NOD-SCID mice by subcutaneous injection. After tumors reached 150–200 mm^3, mice were randomized to receive PU-H71 or vehicle control (4 mice/cohort). PU-H71 was administered daily by intraperitoneal injection at a dose of 50mg/kg for 10 days. This dose was chosen based on a pilot experiment where we evaluated BL xenografts treated at 75mg/kg IP daily, as previously reported (31,32), and 50mg/kg IP daily and found similar efficacy with both doses. Mice were monitored daily for evidence of toxicity and measurement of tumor volume. Mice were sacrificed once tumors reached 3000mm^3. To evaluate tumor growth over time we calculated both tumor volume as well as tumor area under the curve (AUC) as previously described (31).

PU-H71 significantly decreased tumor growth relative to vehicle control in Namalwa bearing xenografts (p=0.0117) (Figure 3A–B). Similar results were seen in a Ramos xenograft model (p=0.0057, Supplemental Fig. 4). There was no evidence of toxicity from PU-H71 based on behavioral evaluation and serial weight measurements. More extensive toxicity profiling has been performed in previous studies including complete blood count, blood chemistry, liver function tests, and thyroid hormone testing with no significant toxicity noted (10,33). This safety profile finding is concordant with that seen in the Phase I clinical study of PU-H71 in patients with previously treated solid tumors, lymphoma and myeloproliferative neoplasms (34).

Since cell line xenografts may not fully recapitulate disease characteristics found in patients, we also evaluated the effect of Hsp90 inhibition in a BL patient derived xenograft (PDX) (Figure 3C–D). Tumor for PDX studies was obtained from a pediatric patient with an

abdominal presentation of Burkitt lymphoma who underwent a biopsy prior to the initiation of therapy. After written informed consent for PDX generation was obtained, surplus primary BL tumor sample was obtained fresh. The tumor was implanted into the subcutaneous flank space of NSG mice. Once tumors reached an approximate volume of 1500 mm^3, the animals (P=0) were euthanized and the tumor removed. This tumor was then separated into 2mm fragments and implanted into (P=1) animals for subsequent drug testing.

We first evaluated PDX tumors to determine if they were similar to the patient tumor phenotype. PDX BL tumors resembled primary BL by histology, immunophenotype, and cytogenetic analysis. The PDX tumors demonstrated the classic starry sky appearance on H&E, had a Ki67 proliferative index >90%, and were positive for CD20 and BCL6 and showed only very weak staining for BCL2, consistent with a BL immunophenotype. In addition, both the PDX and the primary tumor harbored the characteristic MYC translocation (Supplemental Figure 5).

To study the effect of Hsp90 inhibition, PDX mice were treated with PU-H71 (n=6) or vehicle (n=6) once tumors reached 150–200mm^3. PU-H71 was given at a dose of 50mg/kg daily ×15 days. Mice were monitored daily for weight, tumor measurements and toxicity. Treatment with PU-H71 resulted in a significant decrease in tumor volume compared to control (p=0.0074) (Figure 3C). PDX mice did not demonstrate any evidence of PU-H71 induced toxicity. The anti-tumor effect of PU-H71 was more pronounced in the PDX model than in either cell line xenograft model, highlighting the differences between cell lines and patient derived tumors.

Proteomic screen reveals the Hsp90 oncoproteome in BL

Given the promising anti-lymphoma activity of PU-H71 in BL models, we wanted to further explore the mechanism of action to better understand Hsp90 dependent signaling networks in BL and to develop rational therapeutic combinations. To evaluate the targets of PU-H71 in BL we performed high affinity capture followed by proteomic analysis (8). Cellular lysates from two BL cell lines (Ramos, Daudi) were incubated with PU-H71 conjugated agarose beads to chemically precipitate Hsp90 complexes. The protein cargo was then subject to SDS-PAGE and proteins were analyzed using liquid chromatography and tandem mass spectrometry (LC-MS/MS). A total of 752 and 1783 Hsp90 client proteins were identified in Ramos and Daudi respectively (Supplemental Table 1). 701 proteins were common to both cell lines.

Ingenuity Pathway Analysis® was used to determine the signaling networks represented by Hsp90 clients in BL. In both cell lines the PI3K/AKT/mTOR pathway was identified among the most highly represented canonical pathways including “PI3K/AKT signaling”; “p70S6K signaling”; “regulation of eIF4 and p70S6K signaling”; and “mTOR signaling” (Supplemental Table 2). Other top hits which are relevant to lymphocyte biology, included “MYC mediated apoptosis”, “EIF2 signaling” and “protein ubiquitination pathway”. To validate the IPA findings, we performed an independent analysis of the common proteins identified in both Ramos and Daudi using the Search Tool for the Retrieval of Interacting Genes/proteins (STRING) with a CI of 0.99. PI3K proteins formed one of the primary clusters identified in this analysis (Figure 4A). Other clusters included the proteasome, the

ribosome, replication machinery, ribonucleoproteins, translation machinery, and the COP9 signalosome. Both the STRING and the IPA analyses demonstrate that PU-H71 is targeting PI3K signaling among other oncogenic pathways in BL.

PI3K/AKT/mTOR signaling pathway proteins are chaperoned by Hsp90 and require Hsp90 to maintain expression

Recent genomic and functional studies in BL indicate that PI3K signaling contributes to lymphomagenesis (4,35). Given that PI3K, AKT, and mTOR signaling were among the top networks identified in our proteomic screen, we explored the relationship between these pathways and Hsp90. We interrogated our proteomic data and found significant enrichment for PI3K proteins including: multiple isoforms of the PI3K catalytic subunit (PIK3CB, PIK3CD, PIK3CG), the PI3K regulatory subunit (PIK3R1, PIK3R4), and downstream elements (MTOR, S6K1, and EIF4E), (Figure 4B). These findings were validated using chemical precipitation with PU-H71 conjugated beads (Figure 4C). Cellular lysates from Ramos and Daudi were incubated with PU-H71 conjugated beads. The protein cargo was then evaluated using immunoblot analysis probing for PI3K pathway proteins. In both Ramos and Daudi, p110β, p110γ, p110δ, p85α, AKT, and eIF4E were precipitated with PU-H71 beads, confirming their role as Hsp90 clients. In contrast, MCL1, which was not identified as an Hsp90 client in our proteomic screen, was not precipitated by the PU-H71 beads.

To determine if PI3K pathway proteins require Hsp90 chaperoning to maintain expression we exposed Ramos and Namalwa cells to increasing doses of PU-H71 and then analyzed protein abundance by immunoblot (Figure 5A). P-mTOR, p70S6K, and AKT demonstrated both time and dose-dependent decrease upon exposure to PU-H71. To determine if this effect was unique to PU-H71 we also tested other small molecule Hsp90 inhibitors. Treatment with CUDC-305 or ganetespib resulted in similar dose-dependent downregulation of PI3K signaling, confirming the dependence of these proteins on Hsp90 (Figure 5B).

To determine if Hsp90 inhibition impacts PI3K/AKT/mTOR signaling *in-vivo* we performed immunohistochemistry on Namalwa xenograft tumors after exposure to PU-H71. NOD-SCID mice were injected with 1×10^7 Namalwa cells and monitored for tumor progression (n=9). Once tumors reached $500mm^3$, mice were randomized 1:2 to vehicle or a single dose of PU-H71 at 100mg/kg. Tumors were harvested 8 or 24 hours after treatment and evaluated by immunohistochemistry. Immunohistochemistry for p-mTOR and p-p70S6K were negative in all cases including control, reflecting the transient nature of phosphorylation of these proteins. 4EBP1, however, which is downstream in PI3K signaling was moderately decreased in the PU-H71 treated mice at the 8-hour time point and markedly decreased by 24-hours (Figure 5C). Of note, we also evaluated Ki67 and TUNEL in this model to determine if the mechanisms of cell death *in-vivo* were consistent with what we observed *in-vitro*. Similar to our *in-vitro* experiments, we observed a decrease in proliferation as evidenced by Ki67 upon treatment with PU-H71, which was statistically significant at 8hrs (Supplemental Figure 6A) and no increase in TUNEL (Supplemental Figure 6B) consistent with a non-apoptotic mechanism for cell death.

Hsp90 inhibition is synergistic with PI3K/mTOR inhibition in BL

Our data suggests that Hsp90 inhibition is effective in BL in part due to the dependence of PI3K pathway proteins on Hsp90 chaperoning. Given this, we were interested in evaluating the effect of isolated PI3K inhibition on BL. PI3K inhibitors can broadly be categorized into a) class I PI3K isoform-specific inhibitors, b) pan-class I PI3K inhibitors, and c) dual class I PI3K/mTOR inhibitors(36). We tested all three classes of PI3K inhibitors in a panel of BL cell lines. Cells were broadly resistant to isoform specific PI3K inhibition with idelalisib/CAL101 (p110δ inhibitor) and IPI-145 (p110δ/γ inhibitor). Cells demonstrated moderate sensitivity to pan-PI3K inhibition with the pan-class I PI3K inhibitor BKM-120 (15). Cells were most sensitive to BEZ235, which targets both mTOR and all class I isoforms of PI3K (16) (Table 1).

We suspected that PI3K inhibition would be most effective in BL when multiple components of the pathway are targeted, which can be achieved by PU-H71 or BEZ235. Based on this, we hypothesized that PU-H71 might synergize with PI3K inhibitors through more robust dual targeting of PI3K signaling and inhibition of possible feedback mechanisms. To test this we evaluated the combination of PU-H71 and PI3K inhibitors in four BL cell lines (Ramos, Namalwa, Daudi, DG-75). Cells were exposed to increasing doses of each drug alone as well as the combination. The combined response at 48 and 72 hours was evaluated using the Chou-Talalay method (37). A combinatorial index (CI) of <1 was considered synergistic. CI of 1 was considered additive and >1 infra-additive. Since cells were resistant to idelalisib and IPI-145, CI could not be calculated for these combinations. The combination of PU-H71 and BKM-120 was additive or synergistic in 3 of 4 cell lines. The combination of PU-H71 and BEZ 235 was additive or synergistic in all 4 cell lines (Figure 6A).

To further evaluate combination therapy with PU-H71 and BEZ235 we established Namalwa bearing xenografts. Once tumors reached 150–200mm^3, mice were randomized to receive PU-H71, BEZ235, the combination, or vehicle (6 mice/cohort). Mice were treated daily with PU-H71 at 50mg/kg delivered by intraperitoneal injection, BEZ235 at 50mg/kg delivered by oral gavage, the combination, or vehicle for 15 days. As single agents both PU-H71 and BEZ235 reduced tumor growth compared to vehicle (p=0.0196 and p=0.0004 respectively). The combination of PU-H71 and BEZ235 resulted in marked tumor growth suppression with minimal or no growth in most cases. The combination of PU-H71 and BEZ235 suppressed BL tumor growth more than vehicle (p=<0.001), PU-H71 alone (p=0.0008) or BEZ235 alone (p=0.0386) (Figure 6B–C).

Discussion

Our work has identified Hsp90 as a novel therapeutic target in Burkitt lymphoma and has expanded our understanding of the function of Hsp90 in BL. We found that BL tumors overexpress Hsp90 and that BL cells are sensitive to inhibition with small molecule Hsp90 inhibitors. Hsp90 plays a crucial role in normal cellular function by supporting the proteome machinery, which is involved in a number of housekeeping activities. In states of cellular stress Hsp90 exists in an active binding conformation, which is distinct from the “housekeeping” Hsp90 species and is uniquely sensitive to small molecule inhibition(8,38).

This unique sensitivity allows for specific targeting of oncogenic signaling pathways with minimal disruption of “housekeeping” Hsp90. Immunoprecipitation with PU-H71 conjugated beads allows specific pulldown of Hsp90-dependent oncogenic protein clients which are required by tumor cells to maintain growth(8,10,29,31). This pulldown likely includes not only proteins that bind directly to Hsp90 but also those in the epichaperome network (co-chaperones, adaptors, and folding enzymes) that are dependent on Hsp90 to maintain the malignant phenotype(11). In this work we utilized the specificity of PU-H71 as an unbiased approach to characterize the Hsp90-dependent chaperome in Burkitt lymphoma. We identified multiple components of the PI3K/AKT/mTOR pathway as Hsp90 clients. We also found other essential pathways in BL to interact with Hsp90 including MYC mediated apoptosis, B-cell receptor signaling, and protein ubiquitination. Our findings highlight the importance of these pathways in BL and provide a unique opportunity to target multiple oncogenic pathways with a single agent.

The PI3K pathway is thought to play a role in BL pathogenesis based on recent genomic and functional studies. Burkitt lymphoma tumors harbor recurrent alterations in *TCF3* and its negative regulator *ID3* which result in tonic B-cell receptor signaling and activation of PI3K (2–4). In addition, a mouse model in which *MYC* and *PI3K* are constitutively active in germinal center B-cells recapitulates the histomorphology and clinical phenotype(35). Despite the apparent biologic dependence on PI3K, we found isolated PI3K inhibition to have only a modest effect in BL. We suspect that the improved anti-lymphoma effect of PU-H71 over isolated PI3K inhibition is due to targeting of not just PI3K but multiple cellular pathways in BL that depend on Hsp90. It is also likely that isolated PI3K inhibition in BL results in activation of feedback loops and alternative survival pathways, which facilitate escape. In contrast, Hsp90 inhibition prevents escape by also inhibiting these feedback and alternative pathways, which are likely to also be Hsp90 dependent.

In aggressive lymphomas such as BL, single agent therapy is unlikely to be curative. Therefore the use of targeted therapies will require rational combinatorial treatment. Here we demonstrate synergy between PU-H71 and dual PI3K/mTOR inhibition in BL. This treatment combination is particularly well suited for clinical application as both categories of drugs are being evaluated in clinical trials in lymphoma and the drugs are not expected to have overlapping toxicities. A phase I study of PU-H71 is nearing completion and phase II studies are being developed. In addition, other next generation Hsp90 inhibitors, which we also found to be effective in BL, are moving towards clinical implementation with minimal toxicity reported to date(39). Dual PI3K/mTOR agents are also in phase I/II trials in lymphoma (NCT02669511, NCT02249429, NCT01991938).

Although the majority of patients with BL in resource rich settings are cured of their disease (>85%), there remain distinct patient subsets for whom outcomes are poor and targeted therapies are needed(40). Specifically, patients with relapsed disease have a poor response to therapy and an expected overall survival of <20%. In addition, patients with endemic BL have an OS ranging from 25 to 62% due to the inability to safely deliver intensive chemotherapy in resource-limited settings(41). Our work suggests that Hsp90 inhibition based treatment might be effective in both settings. The sensitivity of chemotherapy and immunotherapy resistant BL cells to Hsp90 inhibition (Raji 2R, Raji 4RH) suggests that this

approach may be effective in relapsed disease. Since we were only able to evaluate two resistant cell lines, additional work on other models of resistant BL (such as PDX mice from refractory cases) will be needed to determine the role of PU-H71 in chemotherapy-resistant disease. With regard to use of this agent in the endemic subtype of BL, we observed an anti-tumor effect in endemic BL cell lines *in-vitro* (Raji, Daudi, Namalwa, Jiyoye) and *in-vivo* (Namalwa) suggesting that Hsp90 inhibition may be a rational approach in sub-Saharan Africa.

In summary our work demonstrates that small molecule inhibition of Hsp90 suppresses PI3K/AKT/mTOR signaling and has robust anti-tumor activity in Burkitt lymphoma. We describe, for the first time, the Hsp90-dependent oncoproteome in BL and identify multiple components of PI3K/AKT/mTOR signaling as Hsp90 clients in this malignancy. Lastly, we identify a novel treatment strategy in BL through dual targeting of Hsp90 and PI3K/mTOR. This approach may offer improved efficacy and reduced toxicity over standard chemo-immunotherapy for patients with Burkitt lymphoma.

Supplementary Material

Refer to Web version on PubMed Central for supplementary material.

Acknowledgments

Financial Information: This work was funded by grants from the National Institutes of Health (R01-CA103646 and R01-CA154288) (E. Cesarman), Lymphoma Research Foundation (L. Giulino-Roth), Hyundai Hope on Wheels (L. Giulino-Roth), St. Baldrick's Foundation (L. Giulino-Roth) and the Leukemia and Lymphoma Society (SCOR 7012-16) (E. Cesarman). G. Chiosis is funded by R01 CA172546 and R01 CA155226.

We thank Susan Mathew, MD for performing FISH analysis on PDX tumor samples for the MYC translocation.

References

1. Giulino-Roth L, Wang K, Macdonald TY, Mathew S, Tam Y, Cronin MT, et al. Targeted genomic sequencing of pediatric Burkitt lymphoma identifies recurrent alterations in antiapoptotic and chromatin-remodeling genes. Blood. 2012; 120(26):5181–4. [pii]. DOI: 10.1182/blood-2012-06-437624blood-2012-06-437624 [PubMed: 23091298]
2. Love C, Sun Z, Jima D, Li G, Zhang J, Miles R, et al. The genetic landscape of mutations in Burkitt lymphoma. Nat Genet. 2012; 44(12):1321–5. [pii]. DOI: 10.1038/ng.2468ng.2468 [PubMed: 23143597]
3. Richter J, Schlesner M, Hoffmann S, Kreuz M, Leich E, Burkhardt B, et al. Recurrent mutation of the ID3 gene in Burkitt lymphoma identified by integrated genome, exome and transcriptome sequencing. Nat Genet. 2012; 44(12):1316–20. [pii]. DOI: 10.1038/ng.2469ng.2469 [PubMed: 23143595]
4. Schmitz R, Young RM, Ceribelli M, Jhavar S, Xiao W, Zhang M, et al. Burkitt lymphoma pathogenesis and therapeutic targets from structural and functional genomics. Nature. 2012; 490(7418):116–20. [pii]. DOI: 10.1038/nature11378nature11378 [PubMed: 22885699]
5. Giulino-Roth L, Ricafort R, Kernan NA, Small TN, Trippett TM, Steinherz PG, et al. Ten-year follow-up of pediatric patients with non-Hodgkin lymphoma treated with allogeneic or autologous stem cell transplantation. Pediatr Blood Cancer. 2013; 60(12):2018–24. DOI: 10.1002/pbc.24722 [PubMed: 24038967]
6. Gross TG, Hale GA, He W, Camitta BM, Sanders JE, Cairo MS, et al. Hematopoietic stem cell transplantation for refractory or recurrent non-Hodgkin lymphoma in children and adolescents. Biol

Blood Marrow Transplant. 2010; 16(2):223–30. S1083-8791(09)00444-3 [pii]. DOI: 10.1016/j.bbmt.2009.09.021 [PubMed: 19800015]

7. Jhaveri K, Taldone T, Modi S, Chiosis G. Advances in the clinical development of heat shock protein 90 (Hsp90) inhibitors in cancers. Biochimica et biophysica acta. 2012; 1823(3):742–55. DOI: 10.1016/j.bbamcr.2011.10.008 [PubMed: 22062686]
8. Moulick K, Ahn JH, Zong H, Rodina A, Cerchietti L, Gomes DaGama EM, et al. Affinity-based proteomics reveal cancer-specific networks coordinated by Hsp90. Nat Chem Biol. 2011; 7(11): 818–26. [pii]. DOI: 10.1038/nchembio.670nchembio.670 [PubMed: 21946277]
9. Chiosis G. Discovery and development of purine-scaffold Hsp90 inhibitors. Current topics in medicinal chemistry. 2006; 6(11):1183–91. [PubMed: 16842155]
10. Cerchietti LC, Lopes EC, Yang SN, Hatzi K, Bunting KL, Tsikitas LA, et al. A purine scaffold Hsp90 inhibitor destabilizes BCL-6 and has specific antitumor activity in BCL-6-dependent B cell lymphomas. Nat Med. 2009; 15(12):1369–76. nm.2059 [pii]. DOI: 10.1038/nm.2059 [PubMed: 19966776]
11. Rodina A, Wang T, Yan P, Gomes ED, Dunphy MP, Pillarsetty N, et al. The epichaperome is an integrated chaperome network that facilitates tumour survival. Nature. 2016; 538(7625):397–401. DOI: 10.1038/nature19807 [PubMed: 27706135]
12. Shrestha L, Patel HJ, Chiosis G. Chemical Tools to Investigate Mechanisms Associated with HSP90 and HSP70 in Disease. Cell chemical biology. 2016; 23(1):158–72. DOI: 10.1016/j.chembiol.2015.12.006 [PubMed: 26933742]
13. He H, Zatorska D, Kim J, Aguirre J, Llauger L, She Y, et al. Identification of potent water soluble purine-scaffold inhibitors of the heat shock protein 90. Journal of medicinal chemistry. 2006; 49(1):381–90. DOI: 10.1021/jm0508078 [PubMed: 16392823]
14. Taldone T, Zatorska D, Patel PD, Zong H, Rodina A, Ahn JH, et al. Design, synthesis, and evaluation of small molecule Hsp90 probes. Bioorganic & medicinal chemistry. 2011; 19(8):2603–14. DOI: 10.1016/j.bmc.2011.03.013 [PubMed: 21459002]
15. Burger MT, Pecchi S, Wagman A, Ni ZJ, Knapp M, Hendrickson T, et al. Identification of NVP-BKM120 as a Potent, Selective, Orally Bioavailable Class I PI3 Kinase Inhibitor for Treating Cancer. ACS Med Chem Lett. 2011; 2(10):774–9. DOI: 10.1021/ml200156t [PubMed: 24900266]
16. Maira SM, Stauffer F, Brueggen J, Furet P, Schnell C, Fritsch C, et al. Identification and characterization of NVP-BEZ235, a new orally available dual phosphatidylinositol 3-kinase/mammalian target of rapamycin inhibitor with potent in vivo antitumor activity. Mol Cancer Ther. 2008; 7(7):1851–63. DOI: 10.1158/1535-7163.MCT-08-0017 [PubMed: 18606717]
17. Ying W, Du Z, Sun L, Foley KP, Proia DA, Blackman RK, et al. Ganetespib, a unique triazolone-containing Hsp90 inhibitor, exhibits potent antitumor activity and a superior safety profile for cancer therapy. Mol Cancer Ther. 2012; 11(2):475–84. DOI: 10.1158/1535-7163.MCT-11-0755 [PubMed: 22144665]
18. Lundgren K, Zhang H, Brekken J, Huser N, Powell RE, Timple N, et al. BIIB021, an orally available, fully synthetic small-molecule inhibitor of the heat shock protein Hsp90. Mol Cancer Ther. 2009; 8(4):921–9. DOI: 10.1158/1535-7163.MCT-08-0758 [PubMed: 19372565]
19. Kim SH, Bajji A, Tangallapally R, Markovitz B, Trovato R, Shenderovich M, et al. Discovery of (2S)-1-[4-(2-{6-amino-8-[(6-bromo-1,3-benzodioxol-5-yl)sulfanyl]-9H-purin-9-yl}et hyl)piperidin-1-yl]-2-hydroxypropan-1-one (MPC-3100), a purine-based Hsp90 inhibitor. Journal of medicinal chemistry. 2012; 55(17):7480–501. DOI: 10.1021/jm3004619 [PubMed: 22913511]
20. Bao R, Lai CJ, Qu H, Wang D, Yin L, Zifcak B, et al. CUDC-305, a novel synthetic HSP90 inhibitor with unique pharmacologic properties for cancer therapy. Clin Cancer Res. 2009; 15(12): 4046–57. DOI: 10.1158/1078-0432.CCR-09-0152 [PubMed: 19509149]
21. Gavrieli Y, Sherman Y, Ben-Sasson SA. Identification of programmed cell death in situ via specific labeling of nuclear DNA fragmentation. J Cell Biol. 1992; 119(3):493–501. [PubMed: 1400587]
22. Lohr JG, Stojanov P, Lawrence MS, Auclair D, Chapuy B, Sougnez C, et al. Discovery and prioritization of somatic mutations in diffuse large B-cell lymphoma (DLBCL) by whole-exome sequencing. Proc Natl Acad Sci U S A. 2012; 109(10):3879–84. DOI: 10.1073/pnas.1121343109 [PubMed: 22343534]

23. Wertz IE, Kusam S, Lam C, Okamoto T, Sandoval W, Anderson DJ, et al. Sensitivity to antitubulin chemotherapeutics is regulated by MCL1 and FBW7. Nature. 2011; 471(7336):110–4. nature09779 [pii]. DOI: 10.1038/nature09779 [PubMed: 21368834]
24. Taldone T, Ochiana SO, Patel PD, Chiosis G. Selective targeting of the stress chaperome as a therapeutic strategy. Trends in pharmacological sciences. 2014; 35(11):592–603. DOI: 10.1016/j.tips.2014.09.001 [PubMed: 25262919]
25. Nanbu K, Konishi I, Mandai M, Kuroda H, Hamid AA, Komatsu T, et al. Prognostic significance of heat shock proteins HSP70 and HSP90 in endometrial carcinomas. Cancer detection and prevention. 1998; 22(6):549–55. [PubMed: 9824379]
26. Uozaki H, Ishida T, Kakiuchi C, Horiuchi H, Gotoh T, Iijima T, et al. Expression of heat shock proteins in osteosarcoma and its relationship to prognosis. Pathology, research and practice. 2000; 196(10):665–73. DOI: 10.1016/S0344-0338(00)80118-1
27. Kretzmer H, Bernhart SH, Wang W, Haake A, Weniger MA, Bergmann AK, et al. DNA methylome analysis in Burkitt and follicular lymphomas identifies differentially methylated regions linked to somatic mutation and transcriptional control. Nat Genet. 2015; 47(11):1316–25. DOI: 10.1038/ng.3413 [PubMed: 26437030]
28. Barth MJ, Hernandez-Ilizaliturri FJ, Mavis C, Tsai PC, Gibbs JF, Deeb G, et al. Ofatumumab demonstrates activity against rituximab-sensitive and -resistant cell lines, lymphoma xenografts and primary tumour cells from patients with B-cell lymphoma. Br J Haematol. 2012; 156(4):490–8. DOI: 10.1111/j.1365-2141.2011.08966.x [PubMed: 22150234]
29. Nayar U, Lu P, Goldstein RL, Vider J, Ballon G, Rodina A, et al. Targeting the Hsp90-associated viral oncoproteome in gammaherpesvirus-associated malignancies. Blood. 2013; 122(16):2837–47. DOI: 10.1182/blood-2013-01-479972 [PubMed: 23943653]
30. Brady G, MacArthur GJ, Farrell PJ. Epstein-Barr virus and Burkitt lymphoma. Journal of clinical pathology. 2007; 60(12):1397–402. DOI: 10.1136/jcp.2007.047977 [PubMed: 18042696]
31. Goldstein RL, Yang SN, Taldone T, Chang B, Gerecitano J, Elenitoba-Johnson K, et al. Pharmacoproteomics identifies combinatorial therapy targets for diffuse large B cell lymphoma. J Clin Invest. 2015; 125(12):4559–71. DOI: 10.1172/JCI80714 [PubMed: 26529251]
32. Nayar, ULP., Vider, J., Goldstein, R., Cerchietti, L., Melnick, A., Chiosis, G., Wang, L., Cesarman, E. A purine scaffold Hsp90 inhibitor (PU-H71) has antitumor activity in KSHV-associated malignanies by supressing vFLIP. presented at the American Association for Cancer Research annual meeting; April 2012;
33. Caldas-Lopes E, Cerchietti L, Ahn JH, Clement CC, Robles AI, Rodina A, et al. Hsp90 inhibitor PU-H71, a multimodal inhibitor of malignancy, induces complete responses in triple-negative breast cancer models. Proc Natl Acad Sci U S A. 2009; 106(20):8368–73. DOI: 10.1073/pnas.0903392106 [PubMed: 19416831]
34. Gerecitano JF, Modi S, Rampal Raajit, Drilon Alexander E, Fury Matthew G, Gounder Mrinal M, et al. Phase I trial of the HSP-90 inhibitor PU-H71. ASCO: J Clin Oncol. 2015; 33(suppl) abstr 2537.
35. Sander S, Calado DP, Srinivasan L, Kochert K, Zhang B, Rosolowski M, et al. Synergy between PI3K signaling and MYC in Burkitt lymphomagenesis. Cancer Cell. 2012; 22(2):167–79. S1535-6108(12)00261-9 [pii]. DOI: 10.1016/j.ccr.2012.06.012 [PubMed: 22897848]
36. Yap TA, Bjerke L, Clarke PA, Workman P. Drugging PI3K in cancer: refining targets and therapeutic strategies. Current opinion in pharmacology. 2015; 23:98–107. DOI: 10.1016/j.coph.2015.05.016 [PubMed: 26117819]
37. Chou TC, Talalay P. Quantitative analysis of dose-effect relationships: the combined effects of multiple drugs or enzyme inhibitors. Advances in enzyme regulation. 1984; 22:27–55. [PubMed: 6382953]
38. Kamal A, Thao L, Sensintaffar J, Zhang L, Boehm MF, Fritz LC, et al. A high-affinity conformation of Hsp90 confers tumour selectivity on Hsp90 inhibitors. Nature. 2003; 425(6956):407–10. DOI: 10.1038/nature01913 [PubMed: 14508491]
39. Sidera K, Patsavoudi E. HSP90 inhibitors: current development and potential in cancer therapy. Recent patents on anti-cancer drug discovery. 2014; 9(1):1–20. [PubMed: 23312026]

40. Giulino-Roth L, Goldman S. Recent molecular and therapeutic advances in B-cell non-Hodgkin lymphoma in children. Br J Haematol. 2016; doi: 10.1111/bjh.13969.

41. Stanley CC, Westmoreland KD, Heimlich BJ, El-Mallawany NK, Wasswa P, Mtete I, et al. Outcomes for paediatric Burkitt lymphoma treated with anthracycline-based therapy in Malawi. Br J Haematol. 2016; doi: 10.1111/bjh.13986.

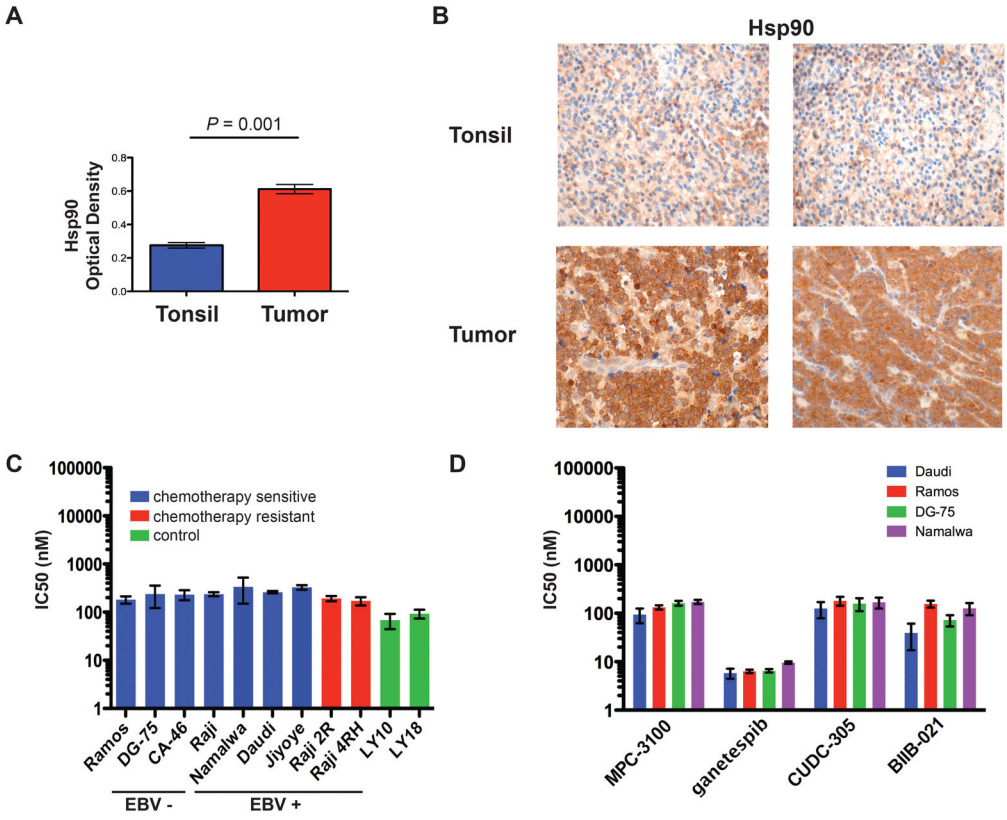

Figure 1. Burkitt lymphomas overexpresses Hsp90 and are sensitive to inhibition with Hsp90 inhibitors *in-vitro*.

(A and B) Hsp90 protein expression as determined by immunohistochemistry in primary BL tumors (n=59) and control tonsil tissue (n=3). Optical density was measured (A) and is shown as average +/− SEM. Panel B shows representative samples of tonsil and BL tumor, original magnification ×600 with 60× objective lens. Microscope: Olympus BX 43; camera: Jenoptik ProgRes CF; software: ProgRes Mac CapturePro 2.7.6. (C and D) IC50 of a panel of EBV-positive and EBV-negative BL cell lines after exposure to PU-H71 or other Hsp90 inhibitors. Cells were exposed to increasing doses of PU-H71, MPC-3100, ganetespib, CUDC-305, BIIB-021 or vehicle control (water + DMSO) and evaluated for viability at 48 hrs using the CellTiter-Glo assay. IC50 was calculated using Prism software (Graphpad). Results represent the mean of 3 biologic replicates, each of which was performed in experimental triplicates. Error bars represent SEM. DLBCL cell lines known to be sensitive to PU-H71 (Ly10, Ly18) were used as positive controls.

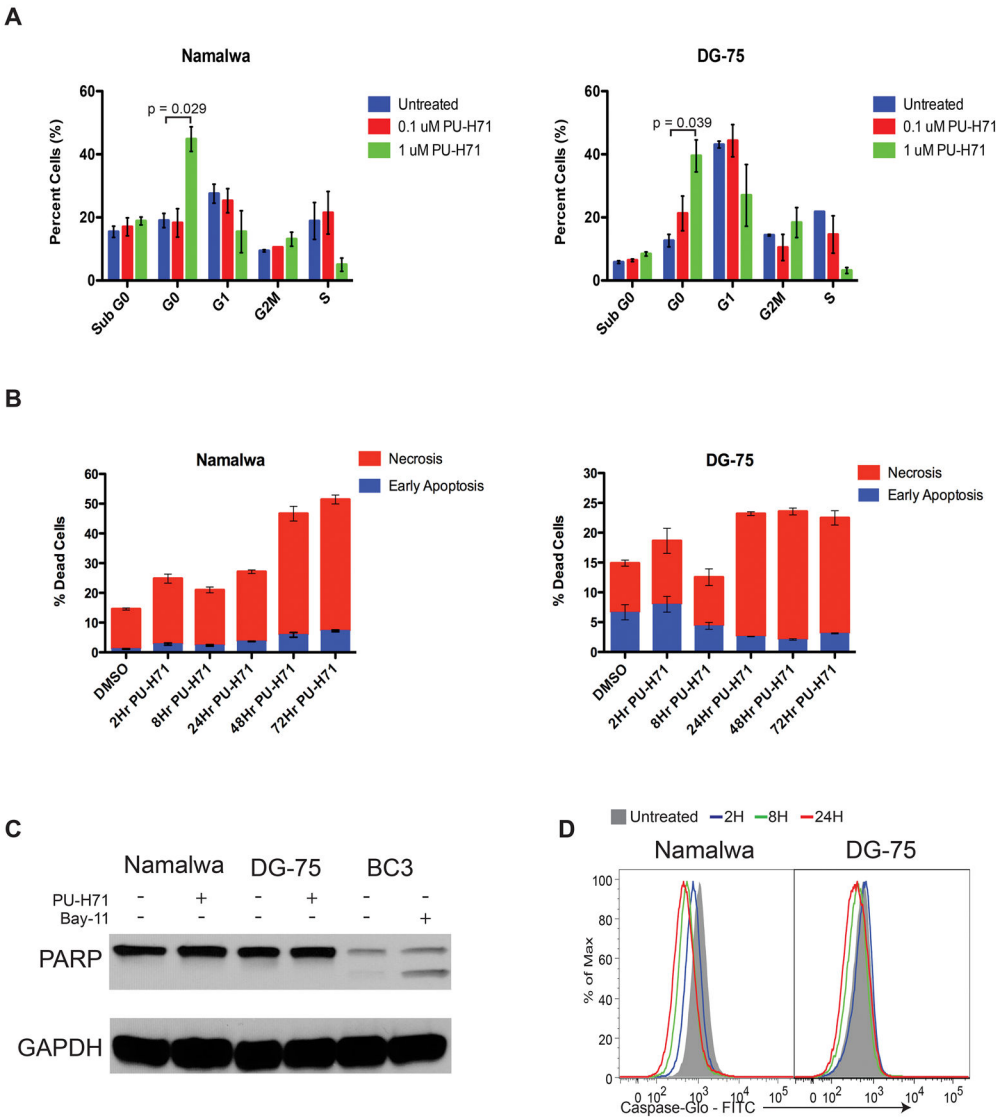

Figure 2. PU-H71 inhibits the growth of BL through cell cycle arrest

(A) Cells were treated with PU-H71 or vehicle control for 24 hours, harvested, fixed and stained with Ki67-BV510 antibody followed by Propidium Iodide (PI) and 1×10^5 cells were analyzed by flow cytometry. The average of three independent experiments are presented with bars representing SEM. (B) Cells were treated with 1μM PU-H71 or vehicle control for 2hr, 8hr, 24hr, 48hr, or 72hr, stained with 7-AAD and Annexin V-AlexaFluor 647 and analyzed by flow cytometry. The average of three independent experiments is shown. (C) Cells were treated with 1uM PU-H71 and evaluated for PARP cleavage at 2hrs. BC3 cells treated with 5uM of Bay11, which is known to induce apoptosis, were used as a positive control. (D) Cells were treated with 1uM PU-H71 at the indicated timepoints. 30 minutes before harvesting, cells were stained with CAS-MAP Green (Intracellular Technologies) working solution. After harvesting, cells were washed and resuspended in PBS for flow cytometry analysis. Cells undergoing apoptosis were detected via fluorescence at 488 nm.

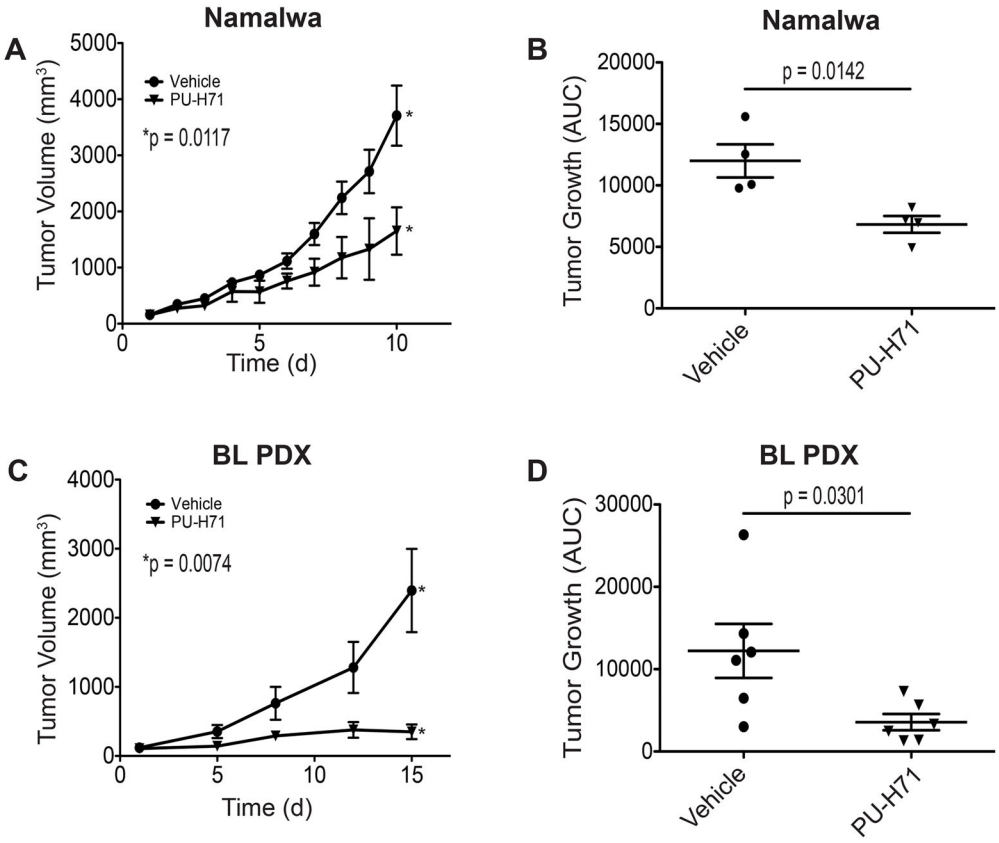

Figure 3. PU-H71 has anti-lymphoma effect *in-vivo*

(A) NOD-SCID mice were injected in the subcutaneous flank with 1×10^7 Namalwa cells. When tumors reached 150–200mm^3 mice were treated with PU-H71 or vehicle control. Tumor growth plot of mice treated with PU-H71 or vehicle control. Error bars represent SEM. (B) Growth of tumor as measured by area under the curve. Average tumor growth is represented on the y axis which represents tumor volume (mm^3)/time (days). Error bars represent SEM. (C) PDX mice were generated using fresh tumor tissue from a patient with an abdominal presentation of BL. Cells were implanted into NSG mice (P0) and once palpable tumors developed, they were fragmented and implanted into additional mice (P1) for further studies. Once tumors reached 150–200mm^3 mice were treated with PU-H71 or vehicle control × 10 days. At the completion of treatment all mice were humanely sacrificed for biology studies. Tumor growth plot of mice treated with PU-H71 or vehicle control. Error bars represent SEM. (D) Growth of tumor as measured by area under the curve. Average tumor growth is represented on the y axis which represents tumor volume (mm^3)/ time (days). Error bars represent SEM.

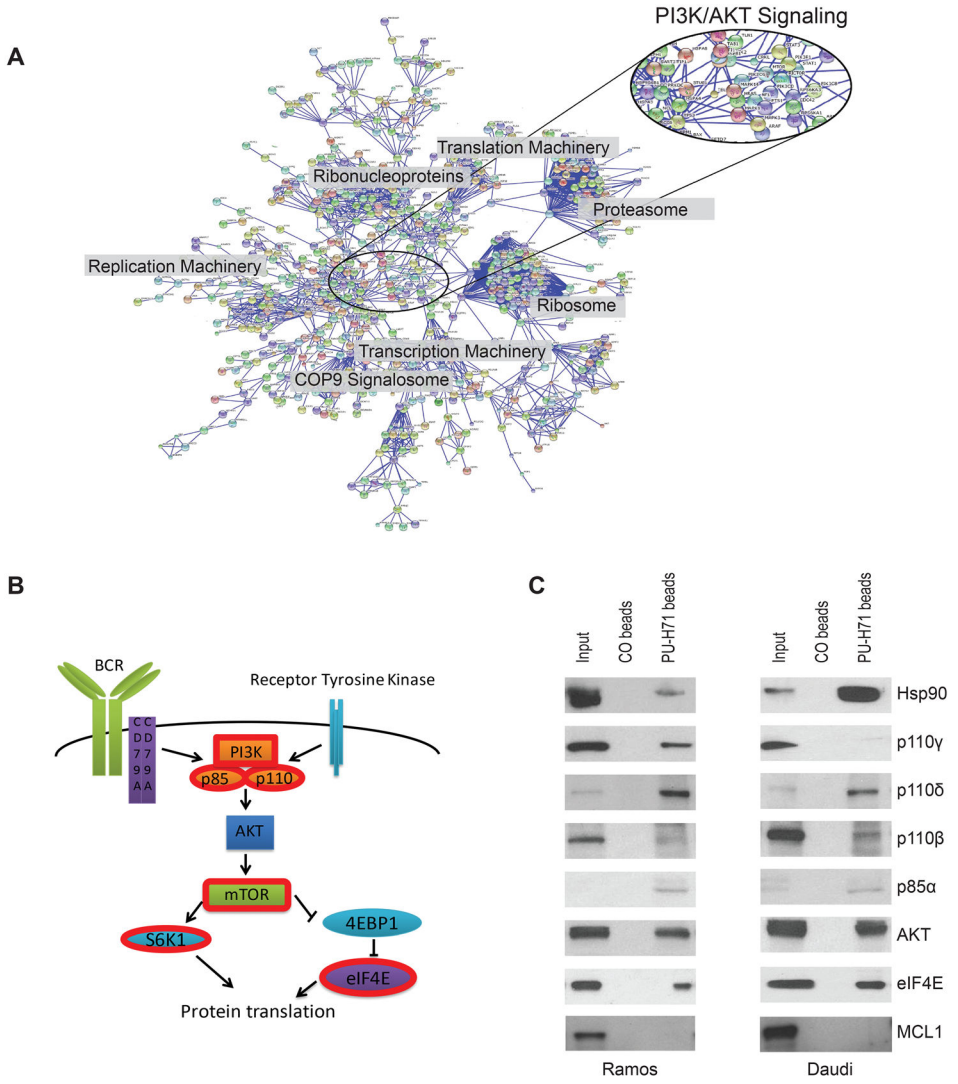

Figure 4. PI3K signaling pathway proteins are Hsp90 clients in BL

(A) STRING representation of the union of proteins identified in Ramos and Daudi chemical precipitations at 0.99 confidence. (B) A representation of the PI3K signaling pathway is shown. Proteins with red borders were identified as Hsp90 chaperone client proteins by LC-MS/MS. (C) Chemical precipitation with PU-H71 conjugated beads: lysates from Ramos and Daudi were subjected to chemical precipitation with PU-H71 conjugated beads or Hsp90-inert control beads (CO) followed by immunoblotting for the indicated PI3K pathway proteins. Hsp90 and MCL1 are used as a positive and negative controls respectively.

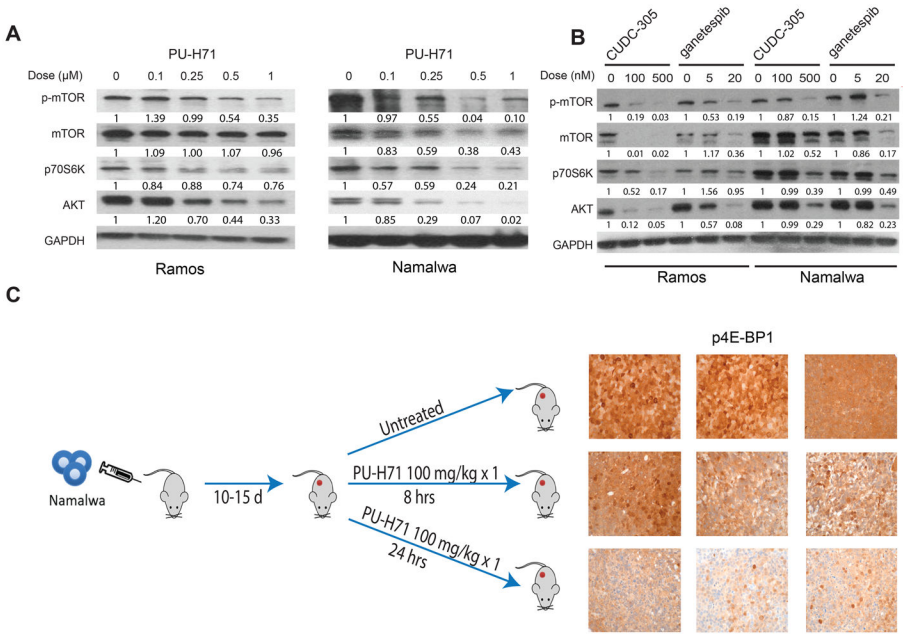

Figure 5. PI3K pathway proteins depend on Hsp90 to maintain expression in-vitro and in-vivo

(A and B) Ramos and Namalwa cells were exposed to PU-H71, CUDC-305, or ganetespib for 24 hours at the doses indicated and evaluated by immunoblot using the indicated antibodies. GAPDH was used as a loading control. Numerical quantification relative to GAPDH and expression in untreated cells is shown below each band (C) Namalwa xenografts were generated by injecting 1×10^7 cells into NOD-SCID mice. 10–15 days after injection, mice were treated with a single dose of PU-H71 at 100mg/kg IP or vehicle control. Mice were humanely sacrificed at 8 or 24 hours after treatment to harvest tumors for immunohistochemistry as indicated. Tumors from 3 mice in each condition (untreated, 8hrs, and 24 hrs) are shown: original magnification ×600 with 60× objective lens. Microscope: Olympus BX 41; camera: Olympus Q-COLOR3; software: QCapture Version 2.9.8.0 (Quantitative Imaging).

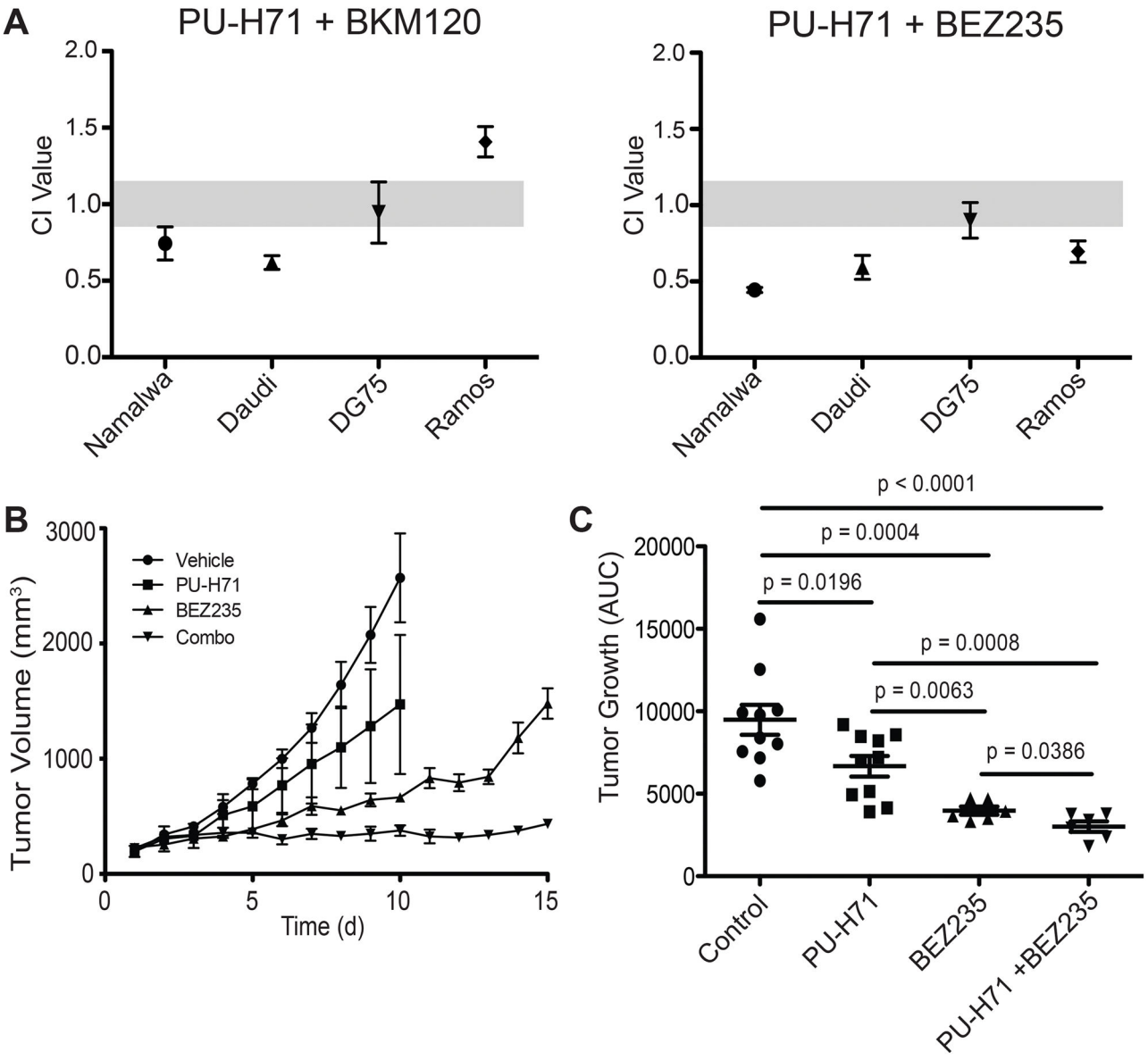

Figure 6. Hsp90 inhibition is synergistic with PI3K/mTOR inhibition in BL

(A) Namalwa, Daudi, DG-75, and Ramos cells were treated with increasing doses of PU-H71 alone, a PI3K inhibitor as indicated alone, or the combination. Cell viability was measured using CellTiter-Glo. Synergy was calculated using Compusyn. CI values <0.9 are synergistic. Results represent the mean of the experiment performed in triplicate +/− SEM. (B) NOD-SCID mice were injected with 1×10^7 Namalwa cells. When tumors reached 150–200mm^3 mice were treated with PU-H71, BEZ235, the combination, or vehicle control. Tumor growth plot of mice treated with PU-H71, BEZ235, the combination, or vehicle control. Error bars represent SEM. (C) Growth of tumor as measured by area under the curve. Average tumor growth is represented on the y axis which represents tumor volume (mm^3)/time (days). Error bars represent SEM.

Table 1

IC50 (nM) of inhibitors of PI3K including isoform specific inhibitors (CAL-101, IPI-145), pan class I inhibition (BKM120) and dual PI3K/mTOR inhibition (BEZ-235). R = resistant.

Cell Line	IC50 (nM)				
	CAL-101 p110δ	IPI-145 p110δ, γ	BKM-120 pan PI3K class I	BEZ-235 PI3K/mTOR	PU-H71
Ramos	R	R	1033	57	181
DG-75	R	R	2009	41	238
Daudi	R	R	2215	35	260
Namalwa	R	R	2602	61	337

Mol Cancer Ther. Author manuscript; available in PMC 2018 September 01.